Geologie en Mijnbouw 66: 121–138 (1987)

Evaporite facies and depositional environment of the Abu Dabbab Formation, Red Sea coast, Egypt

Sanaa Abdel Wahab[1] & Sayed Mahfouz Ahmed[2]
[1] *Department of Geology, Cairo University;* [2] *Department of Geology, Benha University.*

Received 22 December 1986; accepted in revised form 20 March 1987

Abstract

The Abu Dabbab Formation is part of a Middle Miocene sedimentary sequence along the Red Sea Coast that is composed of evaporites with some clastic and carbonate intercalations. These rocks extend for hundreds of kilometres in variable thicknesses and are capped by a fractured and brecciated limestone with surficial calcareous crusts of caliche type.

Detailed field and petrographical studies helped in establishing ten lithofacies types within the Abu Dabbab Formation, mainly evaporites with some dolostones along the upper part of the sequence.

These lithofacies types represent different subenvironments probably indicative of a coastal tidal flat that was intermittently flooded by the sea, thus creating shallow brine-filled depressions or ponds.

There is evidence of alterations in the evaporites brought about by diagenetic processes that were associated with changing environmental conditions.

The diagenetic sequence could be subdivided into three stages: (1) a pre-burial early stage, (2) a burial stage and (3) an uplift late stage.

Introduction

The Middle Miocene rocks in the area between Quseir and Mersa Alam along the Red Sea coastal plain (Fig. 1) consist of a clastic carbonate sequence (Gebel El Rusas Formation) that is covered by an evaporite sequence (Abu Dabbab Formation).

Field investigations and a detailed petrographic study of the mineralogy, fabric and texture of the Abu Dabbab evaporites allowed the recognition of ten facies types, mainly evaporites and some carbonates. We also studied the alterations of these deposits and interpreted the environments which brought about this diagenesis.

The distribution of the different evaporitic facies types fits a model similar to that proposed by Butler (1969, 1970), who subdivided a sabkha flat on the Trucial coast into five zones, where the major controlling factors are the frequency and the extent of flooding: an intertidal zone, an inner, an intermediate and an outer flood recharge zone, and a high supratidal zone. Brine-filled depressions or hypersaline pools have developed on the coastal sabkha flat as in the present day sabkha in the Gulf of Suez (Sellwood & Netherwood, 1984), where gypsum is precipitating subaqueously. These depressions are flooded during storms. The evaporite sequences are generally comparable with those presently accumulating marginal to the Gulf. Intermittent flooding along the coastal flat recharged the pools and delivered seawater to the surface of the sabkha. This, and the downward percolation of the brines caused the development of brine filled pools as well as formation of evaporite minerals and dolomitization of the carbonate sediments.

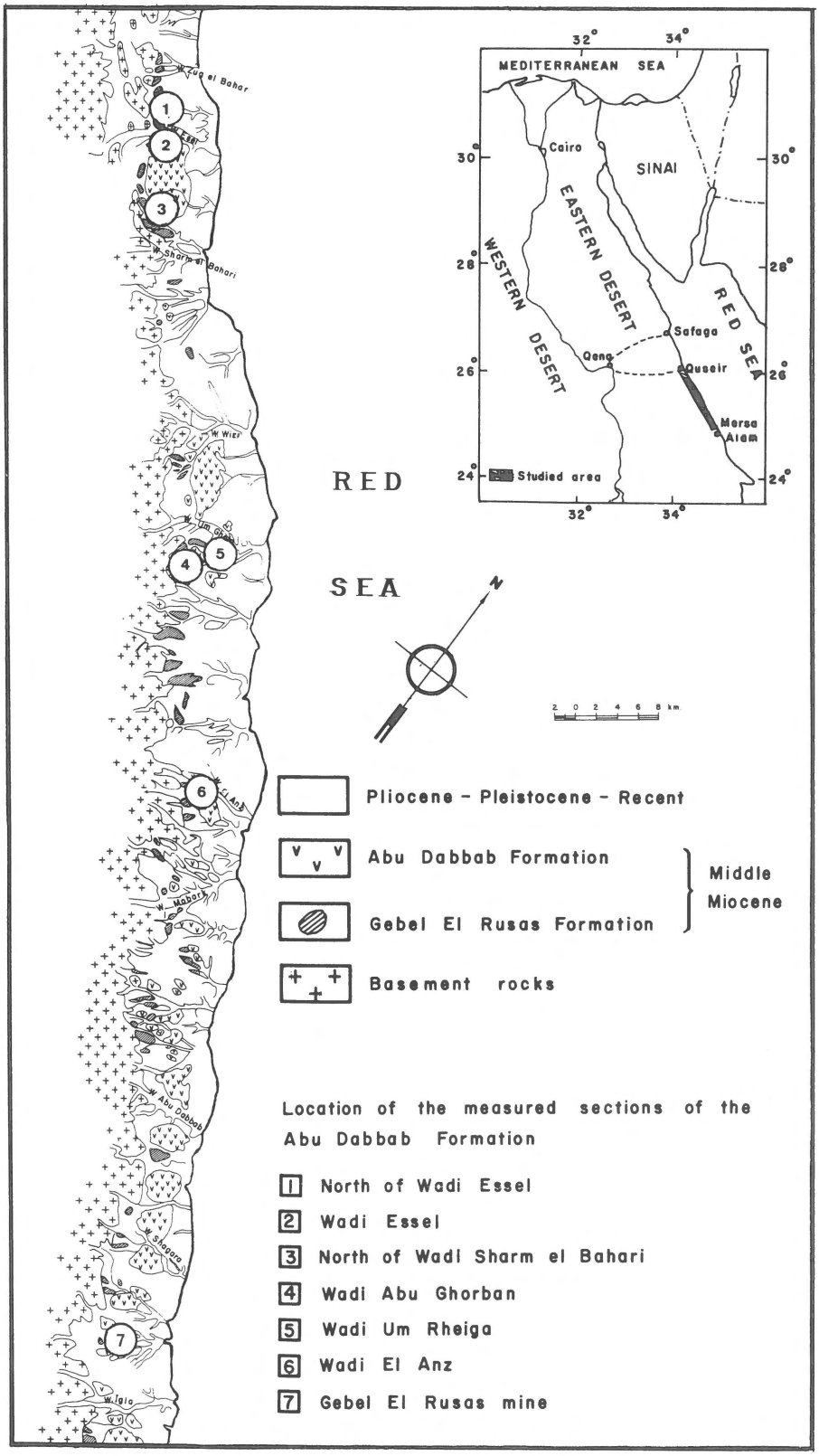

Fig. 1. Geological map of the Red Sea coastal zone between Quseir and Mersa Alam.

Geologic setting

The Red Sea coastal plain is covered by a sedimentary sequence which unconformably overlies Precambrian basement rock. It is represented by Miocene, Pliocene and Pleistocene sediments (Fig. 1). Abu Dabbab evaporites are of Middle Miocene age. The stratigraphy of the Miocene rocks is based on the classification of the National Stratigraphic Sub-committee 1974. The Middle Miocene rocks include the Gebel El-Rusas Formation and the younger Abu Dabbab Formation (Beadnell, 1924; Said, 1962; Akkad & Dardir, 1966).

The Abu Dabbab Formation, extends over hundreds of kilometres along the Red Sea coast. Its thickness is variable. Mostly it does not cover the Gebel El-Rusas Formation but lies at the same level indicating that faulting and uplift occurred after deposition of the Gebel El-Rusas, before deposition of the Abu Dabbab evaporites.

The Gebel El-Rusas Formation is formed of a lower clastic and an upper carbonate member. The clastic member consists of a foreshore/shoreface quartz arenite that is overlain by conglomeratic sediments representing alluvial fan deposits. The carbonate upper sequence consists of dolostones, lime mudstones, reefal, oncolotic and skeletal rocks which are interpreted as deposited on a supratidal, intertidal and reefal environment.

The Abu Dabbab Formation consists of gypsum and anhydrite with some carbonate intercalations in the upper part. Due to dissolution, it is characterized by cone shape hills, cavities and erosional surfaces. The upper parts of this Formation are capped by a fractured and brecciated limestone with calcareous caliche type crusts (El Aref et al., 1985). Earlier descriptions of the Abu Dabbab evaporite can be found in Akkad & Dardir (1966), Issawi et al. (1971), the National Stratigraphic subcommittee (1974), Abu Khadra & Abdel Wahab (1978), El Haddad (1984), Abu Khadra & Youssef (1983) and Youssef (1986).

Petrography and environment of deposition

The petrographic analyses as well as the megascopic features of these evaporites in the seven localities studied, led to the recognition of ten lithofacies units (Fig. 2), from bottom to top:

1. Nodular calcium sulphate with clastic sediments.
2. Nodular stellate evaporite.
3. Thinly bedded anhydrite.
4. Laminated anhydrite.
5. Anhydrite micrite with secondary selenitic gypsum, sulphur and pyrite.
6. Nodular laminated calcium sulphate.
7. Massive alabastrine gypsum.
8. Marly limestone.
9. Dolostone.
10. Dolomitized grainstone.

In the next paragraphs (1–10), the description of each of these units is followed by an interpretation of the environment of deposition.

(1) Nodular calcium sulphate within clastic sediment

This facies is recorded in the lower part of Abu Dabbab Formation. Thicknesses range from 1 to 1.5 m. It consists of green to brown silty shale with dark streaks of possible organic origin. Evaporite laminae are usually intercalated and some anhydrite nodules are found that have displaced the clastic sediments. Under the microscope the nodules are seen to consist of epigenetic felty anhydrite (after gypsum). They form small, irregular and curved lamellae with some impurities. The clastics consist of silt and clay with rare sands. Some fractures and cavities are completely filled with felty anhydrite.

Depositional environment.

The clastic sediments, probably supplied by occasional floods and wind, might have been deposited in an upper intertidal zone and they are definitely associated with traces of algal mats. Gypsum was probably precipitated beneath these algal mats in a manner as reported to occur in Abu Dhabi by Bush (1973). In the upper intertidal zone any drop in sea level will cause these sediments to laterally prograde into a sabkha, inducing dehydration of gypsum into anhydrite. The nodules are thus formed by alteration of the earlier formed gypsum crystals.

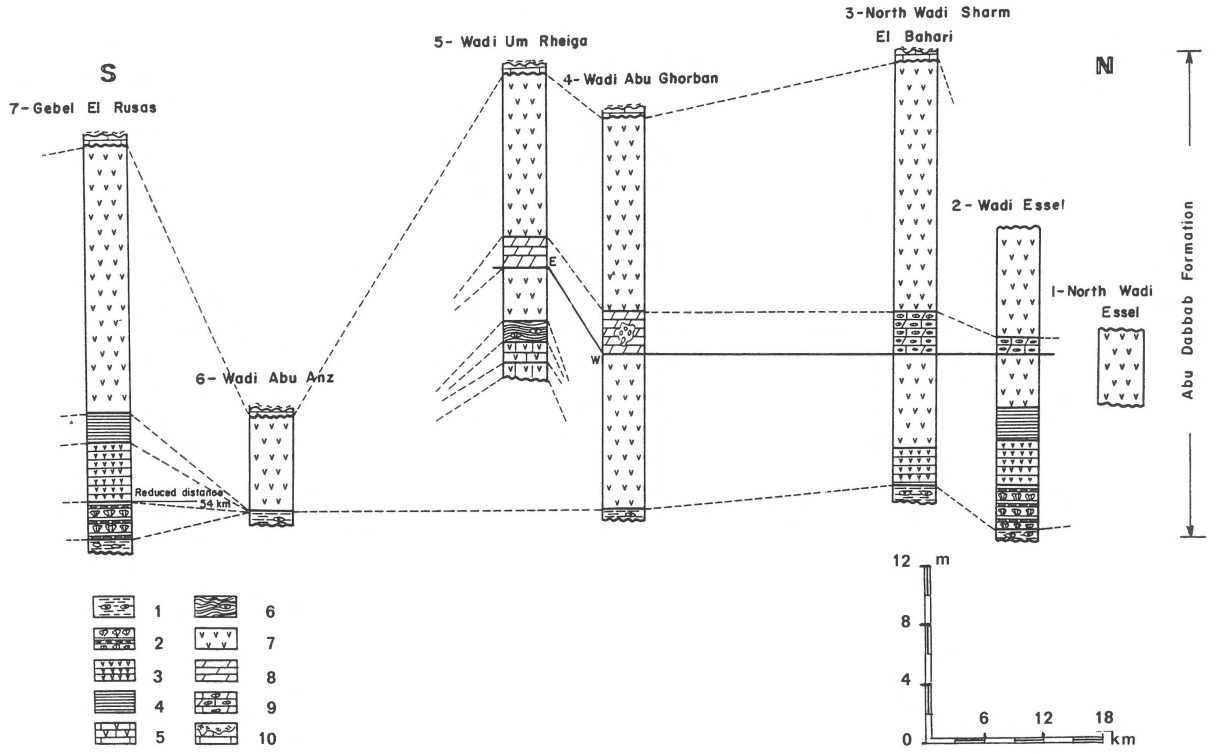

Fig. 2. Lithostratigraphic correlation of the different measured sections of the Abu Dabbab Formation in the area between Quseir and Mersa Alam. Site localities are marked in Fig. 1. Key to lithostratigraphic legend: 1. Nodular calcium sulphate within clastic sediments; 2. Nodular stellate evaporite; 3. Thinly bedded anhydrite; 4. Laminated anhydrite; 5. Anhydrite micrite with selenitic gypsum; 6. Nodular laminated calcium sulphate; 7. Massive alabastrine gypsum; 8. Dolostone; 9. Dolomitized grainstone; 10. Marly limestone capped by calcareous crust of caliche type.

(2) Nodular stellate evaporite

This facies is recorded above the previous one with a thickness up to 3 m. (Fig. a, Plate I). It shows a rhythmic repetition of 3 different layers (Figs. b & c, Plate I): (a) a marly evaporitic layer with characteristic anhydrite nodules, exhibiting a stellate structure; (b) a greenish micritic layer with algal filaments & some oncolites and (c) a halite layer.

a) The powdery whitish marly evaporitic layer is 30 to 60 cm thick. It includes nodules of anhydrite having a fibroradiating or stellate structure. In many places these nodules coalesce and the host rock is only present as discontinuous streaks in between.
b) The greenish micritic layer is very thin (2.5 cm). It overlies the nodular anhydrite and is followed by the halite layer. It includes algal filaments and oncolites and is highly porous with evaporite filling some of the pores.
c) The snow-white halite layer (5–10 cm thick) is continuous for tens of metres, is plane or slightly curved with some voids.

Under the microscope the marly material exhibits some microrhythmic variations that were formed by the deposition of three main geometric elements (Fig. d, Plate I): (1) marly argillaceous material, (2) barite crystals and (3) felty anhydrite.

1. The marly argillaceous layer includes fine, brown laminations of possible organic origin.
2. The barite crytals occur as euhedral crystals or in clusters that grow above the upper surfaces of the marly argillaceous layer, showing a geopetal growing structure. These barite crystals may exhibit idiomorphic terminations towards the next anhydrite layer.
3. The anhydrite layer is composed of epigenetic felty anhydrite after gypsum. The anhydrite

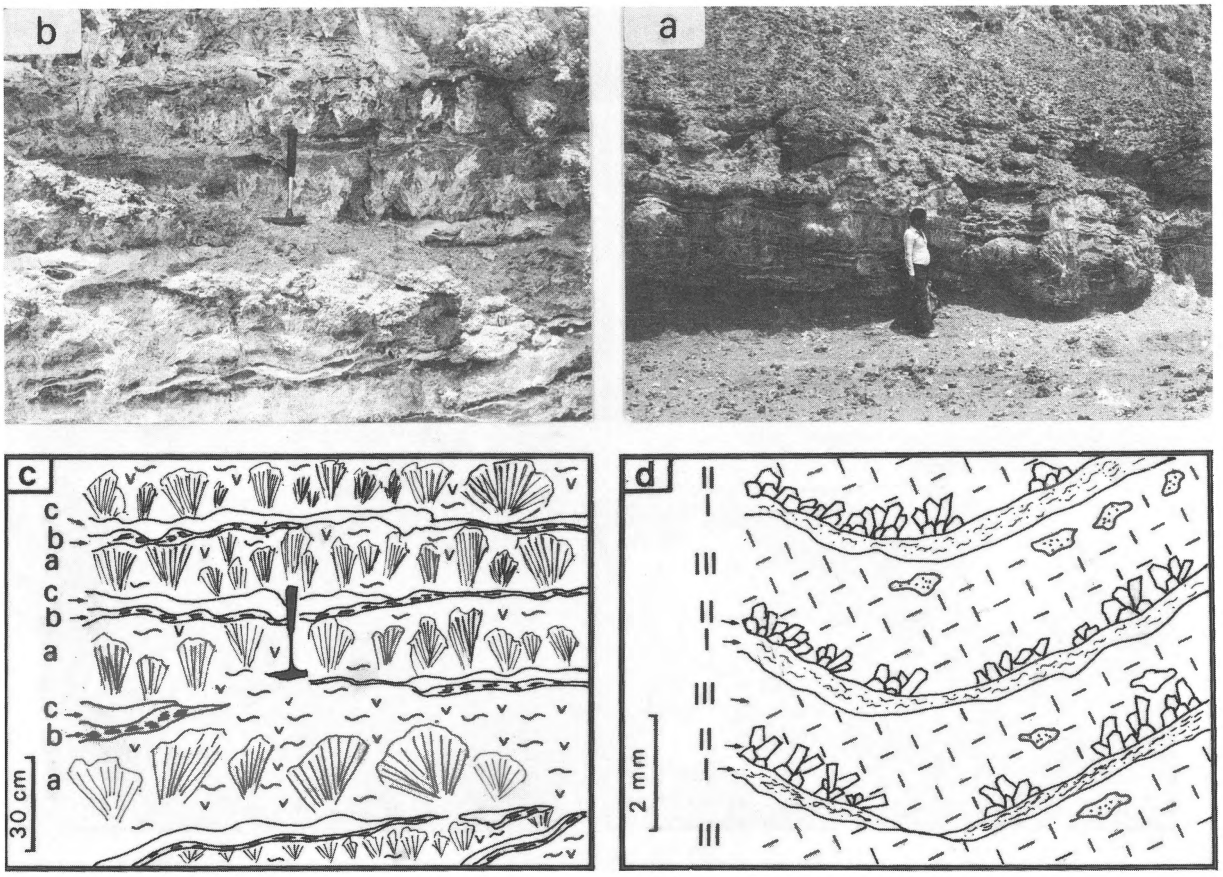

Plate I

a: Stellate nodular evaporitic facies at Essel showing rhythmic repetition of three different layers, marly evaporitic layers with stellate anhydrite nodules, dark greenish micritic layers, and white halite layers.

b: Close-up photograph showing rhythmic deposition of marly evaporitic layers with stellate anhydrite nodules, dark greenish micritic layers and white halite layers.

c: Schematic drawing showing small scale cycles with a rhythmic repetition of (a) marly evaporitic layers with stellate anhydrite nodules, (b) dark greenish micritic layers with oncoids and (c) white halite layers.

d: Schematic drawing of the marly evaporitic layer under the microscope showing microrhythmic repetition of the three generations. Generation I, marly argillaceous layers with organic materials. Generation II, fine to coarse grained barite crystals. Generation III, felty anhydrite and disseminated calcite crystals.

crystals are small with random orientation. Agglomerates of calcite crystals are usually distributed with this layer.

Under the microscope the stellate anhydrite nodules of layer (a) display small, irregular lamellae of felty anhydrite in which rod-like, spindle-shaped crystals are intergrown in a felted network. Many of these lamellae are curved and/or straight and show undulating extinction. The elongation of the anhydrite lamellae is striking and probably results from the unobstructed freedom of growth offered by the wide areas of gypsum in which the anhydrite crystals are randomly arranged (Ogniben, 1957). Some well defined and usually coarsely crystalline gypsum occurs either as isolated crystal or as aggregates in the form of radiating rosette (Figs. a and b, Pl. II). These gypsum crystals have corroded edges indicating the secondary origin of the felty anhydrite crystals.

The green micritic layer (b) contains dark brown algal filaments and rounded oncolites with diameters up to 0.2 mm (Fig. c, Pl. II). Voids partly filled

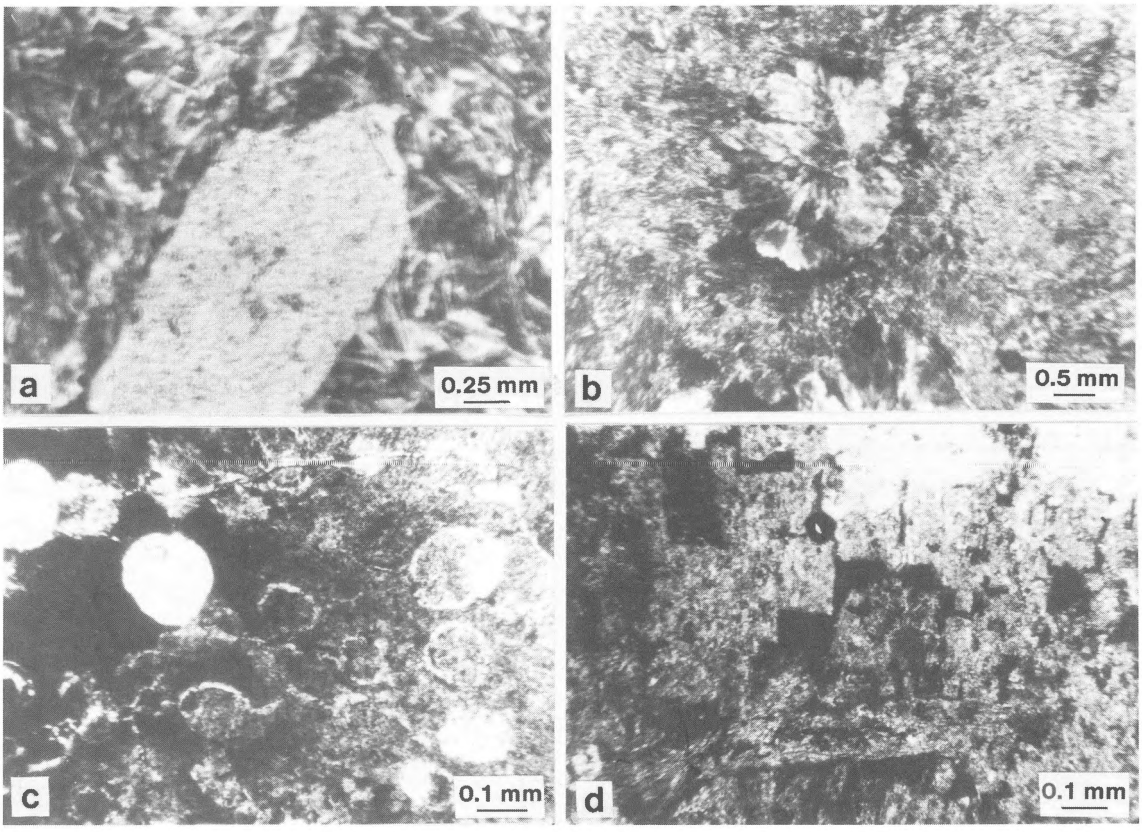

Plate II

a: Isolated crystals of crystalline gypsum embedded within the epigenitic felty anhydrite, having corroded embayed edges in the stellate anhydrite nodules.

b: Gypsum aggregates in the form of radiating rosettes embedded within the epigenitic felty anhydrite in the stellate anhydrite nodules.

c: Rounded oncolite molds, partly or completely filled with micritic material, embedded within the micritic matrix.

d: Large cubes of halite with hopper-like pyramidal hollows.

with anhydrite are observed.

Under the microscope, the halite layer (c) shows pyramide-shaped hopper crystals associated with felty anhydrite crystals (Fig. d, Pl. II).

Depositional environment

The stellate evaporite nodules represent a displacive precipitation stage of evaporite in a coastal sabkha environment. Gypsum is precipitated displacively within the clastic sediments as euhedral and rosette crystals similar to those forming in Texas the Trucial coast (Masson, 1955; Shearman, 1966; Butler, 1970; Bush, 1973) in an intertidal environment. Increasing evaporation leads to a high concentration of the brines, and the gypsum, in contact with the brines, dehydrates into anhydrite. This is then followed by precipitation of more anhydrite on the earlier formed nucleii.

The micrites with their algal filaments and oncolites are upper intertidal deposits (Logan et al., 1974; Schreiber et al., 1976).

The halite bands were deposited subaqueously in a cumulative phase, most probably along the outer flood recharge zones where the brines are saturated with sodium chloride (Butler, 1969). Shearman (1970) has reported layered halite to form in shallow brine-filled depression on supratidal flats in Baja, California.

(3) Thinly bedded anhydrite

This facies is widely distributed in the area with a thickness ranging from 2.5 to 5 m. The evaporites are white, bedded anhydrite (10–40 cm thick), regularly intercalated with thin laminae of fine clastic material (1–3 cm). (Fig. a Pl. III). Under the microscope, the anhydrite appears to be composed of randomly oriented crystals, that are interlocked in a felty network (Fig. b, Pl. III). They contain some clay impurities with barite crystals. Few isolated, euhedral gypsum crystals are disseminated within the anhydrite groundmass. They exhibit embayed, corroded edges indicating the secondary origin of anhydrite. The clastic laminae consist of clay and silty quartz.

Depositional environment
The bedded anhydrite beds are continuous for long distances and are regularly interbedded with thin clastic layers. Friedman (1972) reported that in areas of intensive evaporation, bedded gypsum accumulates in sea-marginal pools like those along today's Red Sea margin. The sediments appear to have been deposited in pools along the intermediate flood recharge zone which is flooded at intervals longer than one month and where the gypsum is reported to be overlain by a skin of detritus. Ultimately this gypsum is progressively replaced by anhydrite (Butler, 1969).

(4) Laminated anhydrite

This facies lies directly above the previous one in the Essel and Gebel El Rusas mine area. The thickness ranges from 1.5 to 2 m. The laminated anhydrite beds are continuous for tens of metres and vary in thickness from 2 to 5 cm, showing a parallel lamination as well as regular intercalations of very thin micritic laminae (Fig. c, Pl. III).

Microscopically, the evaporite consists of mainly epigenetic fine felty anhydrite laths (0.3 mm in size) displaying a very pronounced parallel arrangement, perpendicular to the bedding (Fig. d, Pl. III). Some anhydrite laths are arranged in bundles, still sub-normal to the bedding. Within each bundle, the anhydrite crystals are parallel to one another. The horizontal bundles are thinner (0.1–0.2 mm) and contain some micritic and clayey impurities. Small euhedral gypsum crystals are also observed.

Depositional environment
This facies is characterized by laminated anhydrite with scarse clastic material. Similar laminated anhydrite has been reported to occur in the Middle Devonian of Western Canada (Davies & Ludlam, 1973). Schreiber & Kinsman (1975) described the gypsum of the Montallegro Formation in Sicily as beds of elongate vertical gypsum crystal showing small scale layering within the crystals themselves, as well as planar and undulatory bedding structures. They suggested that this laminated gypsum appears to have been formed by direct precipitation from shallow standing bodies of brine. Similarly, laminated gypsum is apparently forming in shallow water embayments along the east coast of India (Venkkarathman, 1965). The laminated anhydrite under study is secondary after gypsum. This gypsum was probably deposited from a highly concentrated brine in pools or depressions on the sabkha flat. Again, with increasing concentration, gypsum will dehydrate to give anhydrite. The very thin laminae of detrital material within the evaporite crystals may represent ephemeral influxes into the gypsum precipitation area from both eolian and flash flood sources.

(5) Anhydrite, micrite with selenitic secondary gypsum, sulfur and pyrite

This facies is recorded only in the Umm Rheiga Area with a thickness of 1.5 m. It is a massive anhydrite/micrite bed, greyish white in colour and including fenestral cavities ranging in size from a few milimetres to a few centimetres. These cavities are filled with selenite together with elemental sulphur, pyrite and some carbonaceous matter (Fig. a Pl. IV) as well as traces of algal filaments. Differently orientated veins cut the rock and are filled with selenite, sulphur, pyrite, carbonaceous matter and carbonate clasts which form a breccia structure

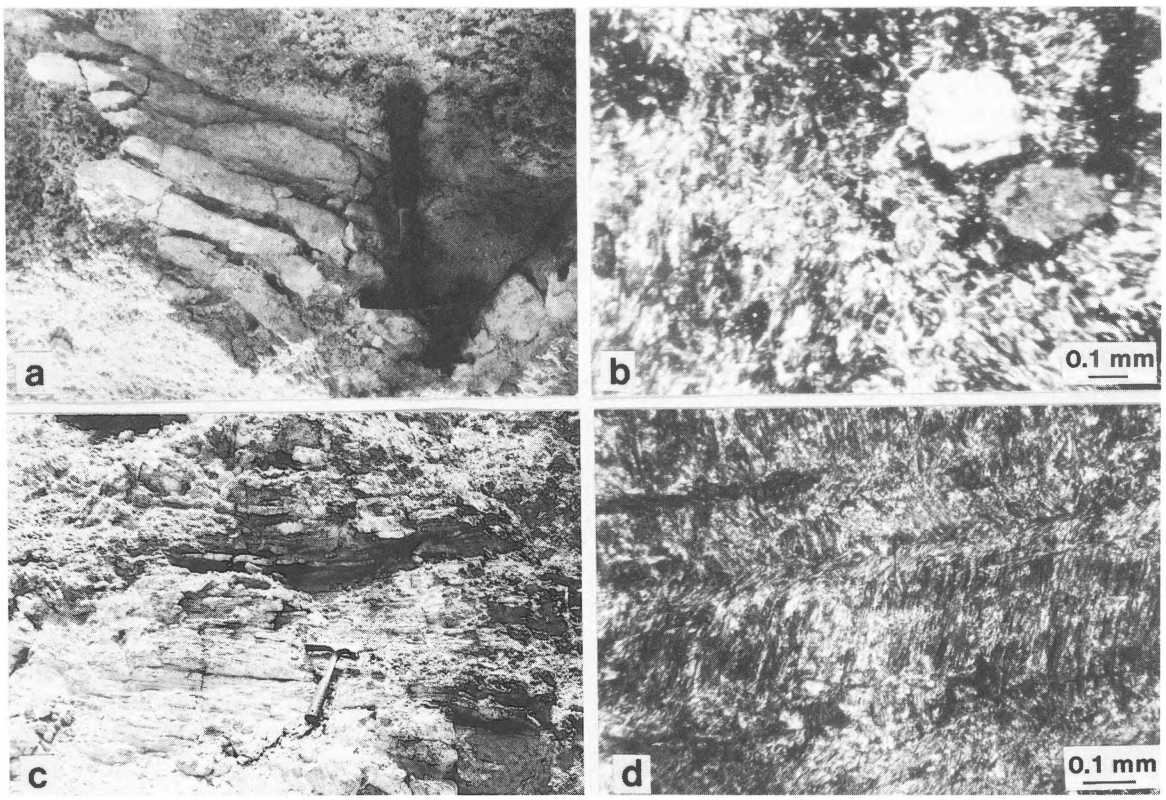

Plate III

a: Thinly bedded anhydrite facies showing regular anhydrite layers intercalated with clastic laminae.

b: Epigenitic felty anhydrite in the thinly bedded anhydrite facies. The anhydrite crystals are random oriented. Corroded isolated gypsum crystals are also observed.

c: Laminated anhydrite facies showing regular lamination.

d: Epigenitic felty anhydrite laths arranged in three different bundles.

(Fig. a, Pl. IV). The elemental sulphur is of a honey yellow to greenish yellow colour which is associated with the selenite occurrences and the organic matter. It is found in the following main megascopic types: (a) disseminated sulphur spots, up to 1 mm in size, distributed along the peripherial lines of the selenite areas; (b) a vein filling type, in which clusters of sulphur grains are deposited along the outer zones of the selenite filled veins; (c) minute sulphur grains are observed along the cleavage planes of selenite crystals and/or included within them.

Under the microscope, the rock consists of micrite together with anhydrite crystals with some dark laminae of possible organic origin. The anhydrite crystals are randomly distributed as isolated elongate crystals up to 0.5 mm in length or they occur as clusters in the form of radiating rosettes. In some instances, the anhydrite crystals are rectangular in shape (Fig. b, Pl. IV), coalescing together to give a 'pile of brick' texture, suggesting that the anhydrite is of primary origin (Goldman, 1952; Ogniben, 1957; Holliday, 1973). Most of the anhydrite crystals are corroded and altered to selenite. The selenite occurs as coarse crystalline aggregates of swallow-tail twins up to a few centimetres in length. Clusters of selenite crystals with ill defined boundaries, forming superindividual polarization grains, are observed with or without limpid cores. These grains may be fibrous and rup-

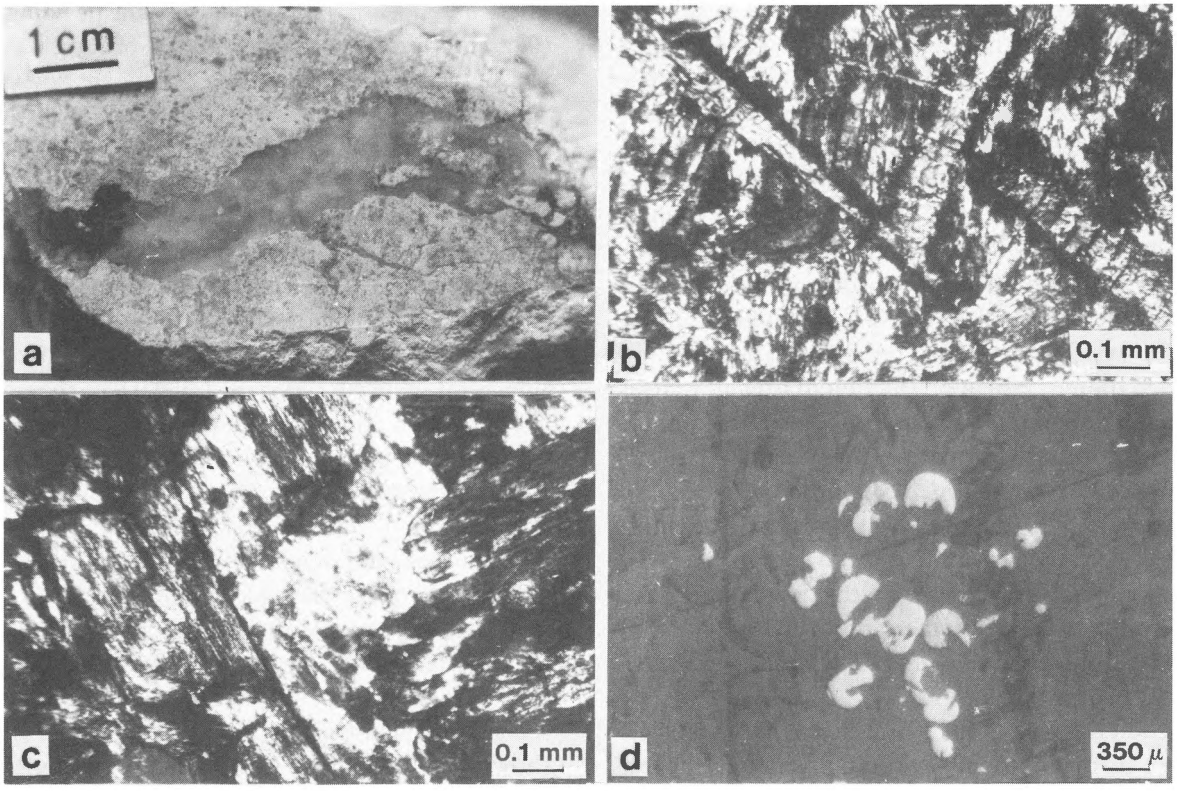

Plate IV

a: Anhydrite-micrite facies with cavities which are filled by white selenitic gypsum, sulphur, pyrite, carbonaceous matter and carbonate clasts.

b: Large anhydrite crystals of anhydrite micrite facies display a very well-realised rectangular outline and form 'pile-of brick' structures.

c: Selenitic secondary gypsum showing limpid core and cloudy superindividual polarization grains, which are ruptured along the cleavage lines.

d: The cellular pyrite forms in the anhydrite-micrite facies are commonly disrupted.

tured along the cleavage lines (Fig. c, Pl. IV). Intergranular fine sized aggregates of selenite crystals are also recorded, which commonly include shreds of anhydrite as well as micrite granules. These inclusions are clear evidence of the secondary origin of the selenite by hydration of the anhydrite.

Pyrite occurs mainly as small spheroids of regular surface up to 300μ in size, filling microcellular organic structures, or rarely as framboidal forms. The internal structures of the framboidal forms are obliterated due to infilling (Love & Amstutz, 1966). The cellular pyrite forms, as well as the sulphur grains are commonly disrupted and pushed aside, most probably by the growing selenite crystals. Fragments of cellular pyrite grains are frequently included and scattered within the selenite (Fig. d, Pl. IV).

Depositional environment

The rock consists of micritic material with fenestral cavities and traces of algal mats which are typical of tidal flat deposits (Laporte, 1967; Shin 1968; Ginsburg, 1975). An arid climate and evaporation of the brines led to the formation of anhydrite within the micritic sediments (Shinn et al., 1969). The anhydrite with a 'pile of bricks' texture, has probably been deposited in the high supratidal

zone in a coastal sabkha. The presence of sulphur may be due to the interaction of organic matter with sulphate-enriched ground waters, the sulphate being reduced by bacterial action. Thus hydrogen sulphide is produced which is then oxidized to elemental sulphur. This is similar to sulphur formation elsewhere. In lake Cyrenaica, Africa (Butlin & Postgate, 1954), precipitation of sulphur proceeds with the participation of both aerobic and anaerobic bacteria. In the Cis-Carpathian sulphur of bio-syngenetic origin is precipitated in lagoons in which there is a high production of organic matter and a highly active bacterial sulphate reduction. In the Montallegro Formation, Sicily, sulphate saturated ground waters, when coming into organic-rich lagoonal waters, induced bacterial activity (Schreiber & Kinsman, 1975). The same goes for the Mishraq sulphur in Iraq, where reduction of evaporites in the presence of bitumen, produced sulphur and calcite during bacterial metabolysis (Barker et al., 1979).

The morphology of pyrite in this facies and its close association with bituminous matter suggest that the pyrite is of syndiagenetic origin formed under reducing conditions by sulphate reducing bacteria. Jackson & Beales (1967) favour the generation of sulphide by sulphate reducing bacteria in the presence of oil or bituminous sediments. Berner (1970, 1971) mentioned that bacterial sulphate reduction is the major source of H_2S and pyrite can form from reaction between dissolved H_2S and iron minerals. Rickard (1975) showed that pyrite normally forms during early diagenesis by the reaction of H_2S derived from bacterial sulphate reduction with fine detrital iron minerals. The sediments of this facies were most probably uplifted and dissected by veins, and anhydrite was hydrated to give secondary selenitic gypsum. This selenite filled the cavities and fractures.

(6) Nodular laminated calcium sulphate

This facies is recorded only in one locality (Um Rheiga area), above the previous one and has a thickness of 1.7 m. It consists of nodular calcium sulphate associated with laminated gypsum and is intercalated with reddish brown clastic laminae (0.5–1 mm). The gypsum laminae occur as thin, parallel layers, 1–3 mm thick, they are uneven, wavy and crenulated. Very thin dark streaks of organic origin are associated with the clastic laminae. Discrete nodules of calcium sulphate usually alternate with the clastic and gypsum laminae. They range in size from 2–5 cm, are elongate in shape and lie parallel to the bedding. Ptygmatic structures are common (Fig. a, Pl. V). Under the microscope, the laminated gypsum is composed of subhedral gypsum crystals (30–80 μ), they are nearly equant and/or elongate in shape. There are no traces of recrystallization, some micrite and some clayey material are disseminated through the gypsum (Fig. b, Pl. V).

Numerous vugs parallel to the boundaries of the laminae are observed, which might have been formed after dissolution of sulphate nodules. The clastic material consists of silt, clay and/or carbonate mud with dark algal streaks. The nodules consist of secondary alabastrine gypsum of the normal type, showing a maximum development of superindividual polarization zones with no definite boundaries between the superindividuals. There are small irregular relicts of anhydrite shreds included within the gypsum.

Depositional environment

The occurrence of uneven laminated gypsum with ptygmatic stuctures and coalescing nodules of secondary gypsum after anhydrite exhibiting a parallel orientation to the bedding is similar to the sulphate bearing sequences in the arid zone of a supratidal sabkha described by Shearman (1966) from the Trucial coast. The anhydrite nodules tend to have formed in layers subparallel to the bedding. With their continuous growth the layers become contorted into ptygmatic structures. It is assumed that the sediments of this facies were deposited in a supratidal environment. The included carbonate material was probably washed onto the supratidal flat at high spring tides (Shearman, 1978). The alabastrine gypsum within the nodules was formed after uplift as the anhydrite was hydrated by meteoric water.

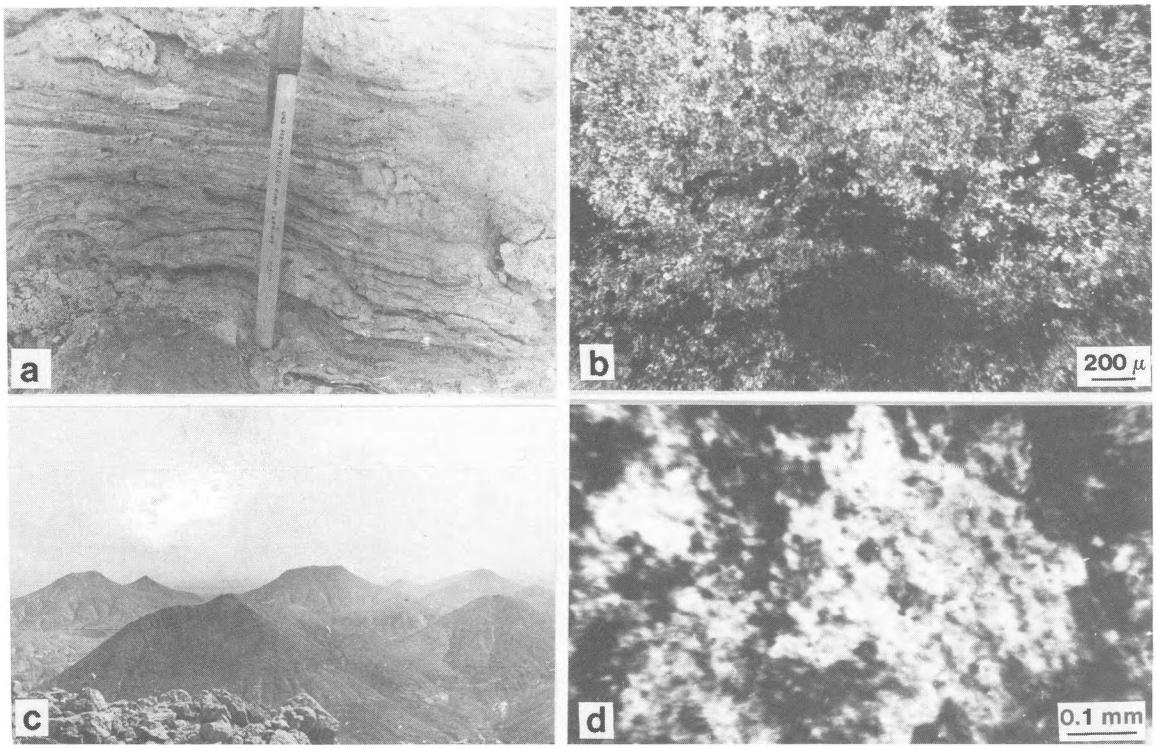

Plate V

a: Nodular-laminated calcium sulphate facies showing ptygmatic structures.
b: Fine subhedral gypsum crystals with disseminated micritic and clayey materials. Different pore spaces are also observed.
c: Massive secondary alabastrine gypsum in the form of conehills, approximately 25 m high.
d: Secondary alabastrine gypsum, normal type, typical 'cloudy' superindividuals.

(7) Massive alabastrine secondary gypsum

This facies is recorded in all the studied sections with a variable thickness of 6–30 m. It is the upper part of the evaporite sequence and forms a chain of conspicuous karst cone hills (Fig. c, Pl. V).

Microscopically, the rock consists of two varieties of secondary alabastrine gypsum: the normal type for the uppermost part, the granoblastic type for the lower part of the facies, respectively. The normal alabastrine gypsum shows a maximum development of superindividuals of a cloudy appearance with no definite boundaries in between, which grade irregularly into one another and may reach several mm in length (Fig. d, Pl. V). Small anhydrite shreds are included within the gypsum as well as clayey impurities, iron oxides and barite crystals. Pseudomorphic calcite after gypsum is observed either as individual grains or in aggregates (Fig. a, Pl. VI). Spherulitic chalcedonic quartz (up to 2 mm in size) is also included within the groundmass, suggesting a filling of voids of dissolved sulphates (Fig. b, Pl. VI).

The granoblastic gypsum that characterizes the lower part, corresponds to the type 2 'hydration' texture of Holliday (1970). It consists of disoriented equidimensional gypsum aggregates associated with anhydrite and normal alabastrine gypsum. The anhydrite is mostly corroded by the granoblasts and is commonly included within it (Fig. c, Pl. VI). The porphyroblastic type of secondary gypsum is missing as are the original textures and structures.

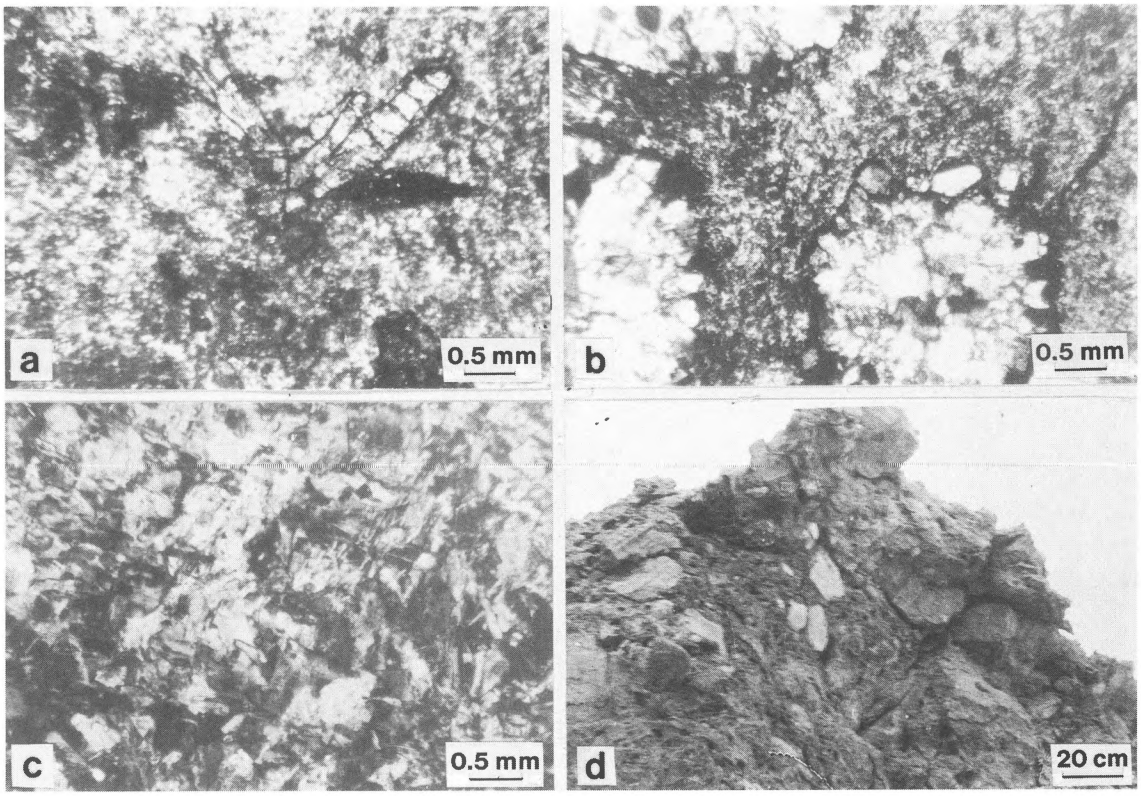

Plate VI

a: Aggregates of pseudomorphic calcite after gypsum in alabastrine gypsum.
b: Spherulitic chalcedonic quartz included within alabastrine gypsum.
c: Granoblastic gypsum of the massive alabastrine gypsum with associated anhydrite and normal alabastrine gypsum type.
d: Highly brecciated marly limestone facies. The fragments are cemented by calcareous crusts of caliche type.

Depositional environment

The primary anhydrite has developed in a supratidal sabkha environment as described by Shearman (1966), conformably within the high supratidal zone of Butler (1969) who reported also the alteration of the preexisting anhydrite to gypsum.

There is clear evidence that gypsum is formed directly by hydration of the anhydrite and this hydration process is more complete in the upper part of the sequence, because the upper part has been more affected by meteoric water. It is believed that hydration took place through dissolution of anhydrite molecule by molecule with precipitation of calcium sulphate ions with water to form gypsum. This mechanism was accepted by the majority of workers (Goldman, 1952, Ogniben, 1957, Holliday, 1970, Mossop & Shearman, 1973) as the most likely process for the natural hydration of anhydrite to gypsum. Schreiber et al. (1976) mentioned the possibility that formation of alabastrine gypsum after anhydrite is probably associated with a very localized tectonically controlled pressure temperature gradient. Under such conditions gypsum dewaters into anhydrite. Alabastrine gypsum of this facies was probably formed by hydration of the preexisting anhydrite by meteoric water introduced from above (Abu Khadra & Abdel Wahab, 1978). This is emphasized by the close relationship between this facies and the exposed karst cone hills of the evaporite sequence and also by the increase in the amount of anhydrite relicts within the lower part of this facies.

(8) Marly limestone

This facies is present in the upper most surface of the Abu Dabbab Formation, directly above the alabastrine gypsum and is overlain by the surficial calcareous crust of caliche type (Fig. d, Pl. VI). The sediments consist of marly micrite with no fauna. The original textures and structures are obliterated through brecciation and the effects of episodic subaerial exposure. The facies is characterized by the development of cone karst features together with dark calcareous crusts and laminae of caliche type (El Aref et al. 1985). The upper horizon, representing the earlier episode of the karst dissolution, exhibits vertical and horizontal karren with cracks and veinlets. A lower horizon with angular and subangular clasts in a silty clay matrix is usually stained with iron and manganese oxides.

Depositional environment

The marly micrite was deposited in association with the primary anhydrite in a sabkha environment along the high supratidal zone. The sediments exhibit all the karst dissolutional features, brecciation and deposition of caliche crusts, which indicate subaerial exposure under arid to semi-arid paleoclimatic conditions during the Pliocene & Pleistocene.

(9) Dolostone

It is recorded in the Gabel Abu Ghorban and Um Rheiga areas, is interbedded within the alabastrine gypsum facies, and has a thickness of 1–3 m. The dolostone is horizontally bedded and has abundant pores and fractures. Black and reddish spots of manganese and iron oxides and snow-white gypsum streaks are recorded. Solution cavities, filled with variable proportions of fragments that are embedded in very fine calcareous material, are observed.

Under the microscope the dolostone is composed of a dark, crystalline dolomite that shows (Fig. a, Pl. VII) a xenotopic to hypidiotopic texture, ranging in size from 20 μ to 40 μ. Pores and vugs are sometimes lined with clear idiotopic larger dolomite rhombs (50–80μ) (Fig. b, Pl. VII). Bird's eyes are partly filled with gypsum.

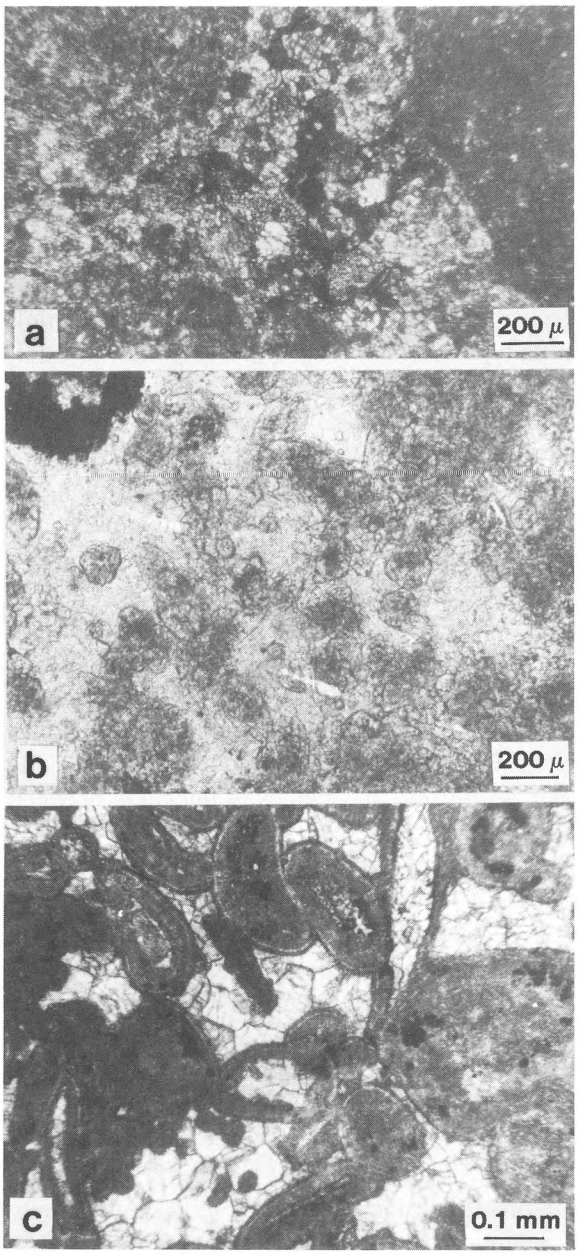

Plate VII

a: Porous cryptocrystalline dolomite crystals of the dolostone facies.

b: Coarse crystalline dolomite rhombs in the wall of the pore-spaces. The pore spaces are filled with gypsum.

c: Dolomitized oncolitic grainstone facies. Blocky calcite crystals fill inter- and intraparticle spaces.

Depositional environment
Roehl (1967) showed that flat breccia is diagnostic of the supratidal zone, while bird's eye structure is interpreted by Schinn (1968) as a common feature in intertidal flat sediments. The size and fabric of the dolomite rhombs resemble closely the penecontemporaneous dolomites that occur in ancient and recent intertidal-supratidal flats. The association of primary structures (fracturing, bird's eye, brecciation), the absence of fauna, and the dolomite type indicate a supratidal origin for this dolostone. After uplift, weathering and karstification, the rock fractures and brecciates, forming semi-rounded solution cavities which are filled with fragments that are embedded in fine, partially consolidated, calcareous material with barite nodules (El Aref & Ahmed, in press).

(10) Dolomitized grainstone

This facies is recorded in Esel and north of Wadi El Sherm El Bahari. It is interbedded within the alabastrine gypsum and ranges in thickness between 1–1.5 m.

Microscopically the rock is a dolomitized grainstone composed for 80% of particles, oncolites, gastropod clasts, bioclast intraclasts that are set in an equant coarse, sparry calcite cement with some evaporite material (Fig. c, Pl. VII). Little detrital quartz is recorded. The particles are partly affected by dolomitization, being well rounded and well sorted.

Depositional environment
The presence of oncolites may indicate that these sediments were deposited in lagoon, intertidal flats or shelf interior where oncolites are generally recorded (Heckel, 1972). Dolomitization took place through an increase in the Mg/Ca ratio of the pore water (Folk & Land 1975). After uplift, meteoric water affects this limestone, initiating the equant cement around the grains. Blocky calcite cement is typical of fresh water cementation.

Diagenesis

The diagenesis of evaporites is complicated because of the continuous changes that are associated with changing environmental conditions. Petrographical studies of the evaporites enabled the interpretation of a diagenetic sequence in 3 different stages (Fig. 3): (1) a pre-burial, early stage; (2) a burial stage; and (3) an uplift, late stage.

(1) Pre-burial early stage

This is the very early stage of diagenesis that is penecontemporaneous with sedimentation. The main factors controlling diagenesis during this stage are the composition of the host sediments, the composition of the brine waters, and the climatic conditions. This stage is characterized by the transformation of gypsum into anhydrite as indicated by the presence of gypsum relicts with corroded, embayed edges within the felty epigenetic anhydrite of the nodular stellate evaporite facies, (2) thinly bedded anhydrite (facies 3) and laminated anhydrite (4). It is analogous to the anhydrite after gypsum that forms today in the Trucial coast (Shearman 1966 & 1978, Kinsman, 1966 & 1969). Fine-grained dolomite (10–40 μ) is also related to this early stage. The size and fabric of these dolomites closely resemble the early penecontemporaneous dolomites that are formed in ancient and recent intertidal to supratidal flats. Laporte (1967), Friedman (1965) and Mossler (1971) have described fine xenotopic, unzoned dolomites forming during the early phase of syngenetic replacement of pre-existing carbonates.

Dolomitization is extensive in the laminated supratidal sediments, whereas the intertidal, algal, oncolotic sediments are only partly dolomitized. This seems to be controlled by the frequency of sea water flooding and the greater permeability towards the inner part of the sabkha where, the algal mats die out (Butler, 1973). The Mg-rich brines that were concentrated by evaporation and solution of soluble salts will percolate downward and dolomitize the carbonate sediments.

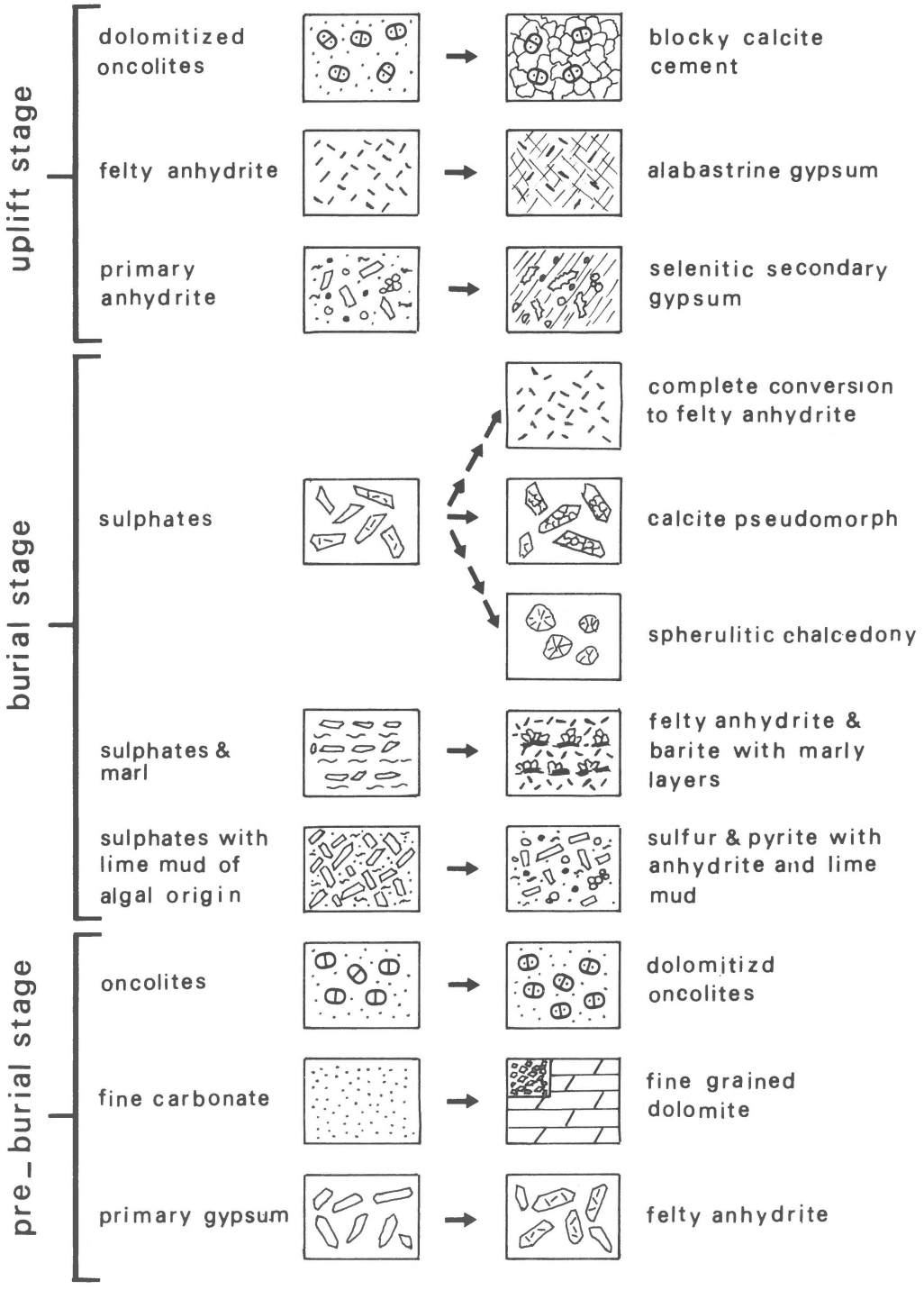

Fig. 3. Diagenetic stages of the sediments of the Abu Dabbab Formation.

(2) Burial stage

This stage includes all the diagenetic processes that took place at shallow and deep burial levels.

Sulphur is formed during the shallow burial, early cementation of the anhydrite-micrite (facies 5) by interaction of the organic matter with sulphate-enriched ground waters. The sulphate ions are reduced by sulphate reducing bacteria and give hydrogen sulphide which is then oxidized to elemental sulphur. Also the pyrite in the same facies was probably formed during this stage under reducing condition, filling the microcellular organic structures or being preserved as framboids.

The barite crystals in the powdery marly evaporitic layers of the nodular stellate evaporite (facies 2), which occur as crystals or clusters along the upper surfaces of the marly layer with a geopetal structure, have a syngenetic origin (shallow burial). The barite crystallizes from saturated barium sulphate solutions that ooze out of the clayey layers under compaction (Zimmerman, 1976).

This stage is characterized by dissolution of some sulphate crystals and by precipitation of silica as spherulitic chalcedonic quartz. The formation of calcite pseudomorphs after gypsum in alabastrine gypsum (facies 7) belongs to a deep burial stage of diagenesis as reported by West (1964). The complete conversion of gypsum into epigenetic anhydrite and the continuous growth of anhydrite crystals as observed in facies 2 and 3 took place during this stage of diagenesis.

(3) Uplift, late stage

Some diagenetic processes occurred after the uplift under the influence of intensive sub-aerial weathering. Such are the formation of selenitic secondary gypsum in the anhydrite micrite (facies 5) and the hydration of primary anhydrite. It is believed that meteoric water has possibly dissolved the calcium sulphate from the main evaporitic material and redeposited it as selenite in the fractures and fenestral cavities. The two varieties of alabastrine gypsum (facies 7), both the normal and the granoblastic gypsum, were formed during this stage by hydration. It is to be noted that anhydrite relicts are more abundant in the base of this facies within the granoblastic gypsum than in the upper normal alabastrine gypsum. This indicates that hydration was more complete along the upper part of the facies which were more exposed to the effect of meteoric water.

The blocky equant calcite mosaic cementing material in the dolomitized grainstone (facies 10) was deposited during this stage. Fresh water, in the phreatic zone, where the meteoric water is saturated with calcium carbonate and is poor in magnesium ions, is the precipitating fluid. The cement is hereby distributed equally around the particles, because the pores are saturated with water (Land, 1970; Longman, 1980).

References

Abu Khadra, A. & S. Abdel Wahab 1978 Origine et pétrologie de la formation de Gypsum, Mersa Alam, Mer Rouge (Egypte). Implications de l'hydrogeologie dans Les autres sciences de la Terre (I.H.E.S. Symposium). Montpellier (France). 11–16 Septembre 1978. Mémoire hors serie CERGH–USTL Montpellier p: 227–239

Abu Khadra, A. & E.A.A. Youssef 1983 Petrography and environment of deposition of Abu Dabbab evaporite, Mersa Alam, Red Sea, Egypt. Teachers' College Bull. V, Kuwait: 37–54

Akkad, S. & A.A. Dardir 1966 Geology of the Red Sea coast between Ras Shagra and Mersa Alam, Egypt. Geol. Surv. Paper 35: 67 p

Barker, J.M.; D.E. Cochran & R. Semrad 1979 Economic geology of the Mishraq native sulfur deposits northern Iraq – Economic Geology, 74, p: 484–495

Beadnell, H.J.L. 1924 Report on the geology of the Red Sea coast between Quseir and Wadi Ranga, Egypt. Min. Fin., Cairo, (Petrol Research Ser.), Bull. 13: 37 pp

Berner, R.A. 1970 Sedimentary pyrite formation – Am. J. Sci., 268: 1–23Berner, R.A. 1971 Principles of chemical sedimentology – McGraw-Hill, New York. 256 pp

Bush, P. 1973 Some aspects of the diagenetic history of the Sabkha in Abu Dhabi, Persian Gulf. In: Purser B.H. (ed.) The Persian Gulf, Holocene carbonate sedimentration and diagenesis in a shallow epicontinental sea: 395–407

Butler, G.P. 1969 Modern evaporite deposition and geochemistry of coexisting brines, the Sabkha, Trucial Coast. Arabian Gulf – Sed. Petrol. 39: 70–89

Butler, G.P. 1970 Holocene gypsum and anhydrite of the Abu Dhabi Sabkha, Trucial coast: An alternative explanation of origin – Third symposium on salt, N. Ohio Geol. Soc.: 120–152

Butler, G.P. 1971 Origin and controls on distribution of arid supratidal (sabkha) dolomite, Abu Dhabi, Trucial coast (abstr.): Bull. Am. Assoc. Petrol. Geol. 55: 332

Butler, G.P. 1973 Strontium geochemistry of modern and ancient calcium sulphate minerals. In: Purser B.H. (ed.) The Persian Gulf, Holocene carbonate sedimentation and diagenesis in shallow epicontinental sea: 423–452

Butlin, K.R. & J.R. Postgate 1954 The microbiological formation of sulfur in Cyrenaican Lakes. In J.L. Cloudsley-Thompson (ed.) Biology of deserts. Inst. of Biology London: 112–122

Davis, G.A. & S.D. Ludlam 1973 Origin of laminated and graded sediments, Middle Devonian of Western Canada – Bull. Geol. Soc. Am. 84: 3527–3546

El Aref, M., S. Abdel Wahab, & S. Ahmed 1985 Surficial calcareous crust of caliche type along the Red Sea coast, Egypt Geol. Rundsch. 74/1: 155–163

El Aref, M. & S. Ahmed, (in press) Diagenetic crystallization rhythmites (DCRs) of dolomite-barite-calcite in karst environment, Gebel Abu Ghorban, Red Sea coastal zone, Egypt – J. Geol. Egypt

El Haddad, A.A. 1984 Sedimentological and geological studies on the Neogene sediments of the Egyptian part of the Red Sea Coast – Ph.D. Thesis, Assiut University: 270 pp

Folk, R.L. & L.S. Land 1975 Mg/Ca ratio and salinity: two controls over crystallization of dolomite – Bull. Am. Ass. Petrol. Geol. 59: 60–68

Friedman, G.M. 1965 Terminology of crystallization textures and fabrics in sedimentary rocks – J. Sed. Petrol. 35, P. 643–655

Friedman, G.M. 1972 Significance of the Red Sea in the problem of evaporites and basinal limestones – Bull. Am. Associ. Petrol. Geol. 56: 1072–1086

Ginsburg, R.N. 1975 Tidal deposits – Springer. Heidelberg, New York: 428 pp

Goldman, M.I. 1952 Deformation, metamorphism and mineralization in gypsum anhydrite cap rock, sulfur salt dome, Louisiana – Geol. Soc. Am. Mem. 50: 169 pp

Heckel, P.H. 1972 Recognition of ancient shallow marine environments. In: J.K. Rigby & W.K. Hamblin (eds) Recognition of ancient sedimentary environments. Publ. Soc. Econ. Paleont. Miner. 16, Tulsa: 226–296

Holliday, D.W. 1970 The petrology of secondary gypsum rocks: a review – J. Sed. Petrol. 40: 734–744

Holliday, D.W. 1973 Early diagenesis in nodular anhydrite rocks – Trans. Inst. Min. Metall. 82: 81–84

Issawi, B., M. Francis, M. El Hinnawy, A. Mehana & T. El Deftar, T. 1971 Geology of Safaga-Quseir coastal plain and of Mohamed Rahba area – Ann. Geol. Sur. Egypt, I: 1–20

Jackson, S.A. & F.W. Beales 1967 An aspect of sedimentary basin evaluation: the concentration of Mississippi Valley type ores during late stage of diagenesis – Bull. Can. Pet. Geol., 15: 383–433

Kinsman, D.J.J. 1966 Gypsum and anhydrite of Recent age, Trucial coast, Persian Gulf – Second symposium on salt. Northern Ohio, Geol. Soc.: 302–326

Kinsman, D.J.J. 1969 Modes of formation, sedimentary association and diagenetic features of shallow water evaporites – Am. Assoc. Petrol. Geol. Bull. 55: 830–840

Land, L.S. 1970 Phreatic versus vadose meteoric diagenesis of limestone: evidence from fossil water table – Sedimentology, 14: 175–188

Laporte, L.F. 1967 Carbonate deposition near mean sea-level and resultant facies mosaic: Manlius Formation (Lower Devonian) of New York State – Bull. Am. Ass. Petrol. Geol. 51: 73–101

Logan, W., P. Hoffman & C.F. Gebelein 1974 Algal mats, crystalline fabrics and structures, Hamelin Pool, Western Australia – Mem. Am. Ass. Petrol. Geol. 22: 14–194

Longman, N.W. 1980 Carbonate diagenetic textures from near surface diagenetic environments – Bull. Am. Ass. Petrol. Geol., 64: 461–487

Love, L.G. & G.C. Amstutz 1966 Review of microscopic pyrite – Fortschr. Mineral., 43: 273–309

Masson, P.H. 1955 An occurrence of gypsum in Texas – J. Sed. Petrol. 25: 72–77

Mossler, J.H. 1971 Diagenesis and dolomitization of Swope Formation (upper Pennsylvanian) south east Kansas. Sed. Petrol. 41: 962–970

Mossop, G.D. & D.J. Shearman 1973 Origins of secondary gypsum rocks – Trans. Inst. Min. Metall. (Section B : Appl. Earth Sci.): 147–154

Ogniben, L. 1957 Secondary gypsum of the sulphur series, Sicily and the so-called integration – Sed. Petrol. 27: 64–79

Rickard, D.T. 1975 Kinetics and mechanism of pyrite formation at low temperatures – Am. Jour. Sci. 275: 636–652

Roehl, P.O. 1967 Stony Mountain (Ordovician) and Interlake (Silurian) facies analogs of Recent low-energy marine (Sic.) and subaerial carbonates, Bahamas – Am. Assoc. Petrol. Geol. Bull. 51: 1979–2032

Said, R. 1962 The Geology of Egypt – Elsevier Amsterdam, New York: 377 pp

Schreiber, B.C.; Friedman, G.M., Decima, A., & Schreiber, E. 1976 Depositional environments of Upper Miocene (Messinian) evaporite deposits of the Sicilian Basin – Sedimentology 23: 729–760

Schreiber, B.C. & D.J.J. Kinsman 1975 New observations on the Pleistocene evaporites of Montallegro, Sicily and a modern analog – J. Sed. Petrol. 45: 469–479

Sellwood, B.W. & R.E. Netherwood 1984 Facies evolution in the Gulf of Suez Area: Sedimentation history as an indicator of rift initiation and development – Modern Geology, 9: 43–69

Shearman, D.J. 1966 Origin of evaporites by diagenesis – Trans. Inst. Min. Metall. 75: 208–215

Shearman, D.J. 1970 Recent halite rocks, Baja California Mexico – Trans. Inst. Min. Metall. 79: 155–162

Shearman, D.J. 1978 Evaporite of coastal sabkhas. In: Marine evaporites – Soc., Ecom. Paleon. Mineral., Short Course No. 4, Oklahoma City: 6–42

Shinn, E.A. 1968 Practical significance of birds eye structures in carbonate rocks – J. Sed. Petrol. 38: 215–223

Shinn, E.A., Lloyd, R.M., & Ginsburg, R.N. 1969 Anatomy of

a modern carbonate tidal flat, Andros Island, Bahamas – J. Sed. Petrol. 39: 1202–1228

Stratigraphic sub-committee of the national committee of geological sciences of Egypt 1974 Miocene rocks stratigraphy of Egypt – Egyptian J. Geol. 18: 11–69

Venkkarathman, K. 1965 Studies on some aspects of the sediments of Chilka Lake (a coastal lagoon): Unpubl. Ph.D. Thesis, Dept. Geology, Andhra University, India. 166 pp

West, I.M. 1964 Evaporite diagenesis in the Lower Purbeck, beds of Dorset – Proc. Yorkshire. Geol. Soc. 34: 315–330

Youssef, E.A.A. 1986 Depositional and diagenetic models of some Miocene evaporites on the Red Sea coast, Egypt – Sed. Geol. 48: 17–36

Zimmerman, R.A. 1976 Rhythmicity of barite-shale and of Sr in strata-bound deposits of Arkansas. In: K.H. Wolf (ed.): Handbook of strata-bound and stratiform ore deposits, 3: 339–353